*Acta Cryst.* (1969). B25, 688

# The Crystal and Molecular Structure of Pyridoxal Phosphate Oxime

BY A. N. BARRETT AND R. A. PALMER

*Crystallography Department, Birkbeck College, London, W.C.1, England*

(*Received* 19 *April* 1968)

The crystal structure of pyridoxal phosphate oxime ($C_8H_{11}N_2O_6P$) has been determined by X-ray single-crystal analysis, and refined by block-diagonal least-squares methods to an $R$ value of 11%. The molecule is planar, with the exception of the phosphate group, and the structure is governed by a complex system of hydrogen bonds. Two of the P–O bonds are normal; the other two, both involved in hydrogen bonding, are abnormally short with bond lengths of 1·48 Å and 1·46 Å respectively. Three methods of preliminary structure determination, symbolic addition, heavy-atom technique, and machine Patterson-superposition, are compared.

## Introduction

Vitamin $B_6$ (I) occurs in three forms in the tissues of animals and plants (Rabinowitz & Snell, 1948), namely (i) pyridoxine in which R≡$CH_2OH$, (ii) pyridoxamine in which R≡$CH_2NH_2$ and (iii) pyridoxal in which R≡CHO. All three forms are converted into the coenzyme pyridoxal phosphate (II) in which R≡CHO, otherwise known as codecarboxylase. The structure determined in the present investigation is that of pyridoxal phosphate oxime ($C_8H_{11}N_2O_6P$), a derivative of codecarboxylase in which R≡CHNOH.

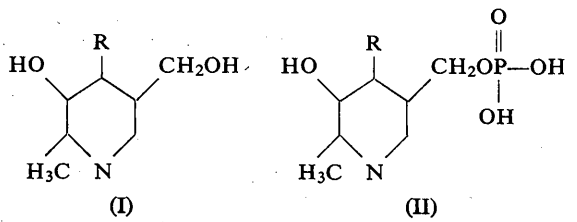


## Experimental

### *Crystallographic data*

The crystals of pyridoxal phosphate oxime are whitish and well developed, with a tendency to elongation in one direction. Preliminary optical and X-ray examination indicated the crystals to be triclinic. The unit-cell parameters, determined initially from oscillation and Weissenberg photographs, were subsequently refined by the least-squares technique of Main & Woolfson (1963). Zero-level $a$ and $c$ axis Weissenberg photographs taken with Cu $K\alpha$ radiation provided 24 suitable $\alpha_1$–$\alpha_2$ doublets for the unit-cell refinement with separations in the range 0·32 to 0·98 mm and a mean error of ±0·02 mm.

The density of the crystals $D_m$ measured by flotation in a mixture of bromo- and iodobenzene was found to be consistent with two molecules of $C_8H_{11}N_2O_6P$ plus two molecules of water per unit cell.

The crystal data are as follows:

Pyridoxal phosphate oxime dihydrate
$C_8H_{11}N_2O_6.2H_2O$
$M=261$
Triclinic
$a=10{\cdot}94\pm0{\cdot}03$ Å,
$b=8{\cdot}06\pm0{\cdot}02$,
$c=9{\cdot}44\pm0{\cdot}03$.
$\alpha=57{\cdot}18\pm0{\cdot}32°$,
$\beta=107{\cdot}68\pm0{\cdot}30$,
$\gamma=116{\cdot}53\pm0{\cdot}27$.
$V=627$ Å$^3$.
$D_m=1{\cdot}57\pm0{\cdot}01$ g.cm$^{-3}$,
$Z=2$,
$D_x=1{\cdot}574$ g.cm$^{-3}$.

Ni-filtered Cu radiation used for intensity and unit-cell measurements, $\lambda=1{\cdot}542$ Å.
$\mu$(Cu $K\alpha$)=24 cm$^{-1}$.
$N_0=1173$ non-zero intensities measured.
Number of unobserved reflexions=395.
70% of radiation sphere explored.
$F(000)=183$.
Space group $P1$ or $P\bar{1}$,
$P\bar{1}$ confirmed by structure analysis.
No required molecular symmetry.

### *Intensity data*

The crystal selected for recording the intensity data was about 0·28 mm long in the **c** direction and 0·15 × 0·12 mm$^2$ in cross-section. Equi-inclination Weissenberg photographs were taken with the crystal rotating about **c** for layers $l=0$ through 7, using a four film pack. Two exposures were made per layer for the rotation ranges 0° to 200° and 180° to 380° respectively, the overlapping regions providing common reflexions for scaling purposes.

The intensities were estimated visually with a calibrated scale prepared by timing a series of exposures from a selected zero-level reflexion. After correcting for Lorentz and polarization factors the levels were scaled together by comparison with common reflexions

on an *a*-axis first level photograph, recorded with a crystal cut from the original specimen.

Errors in the intensity measurements were estimated at about ±10% for strong and medium range intensities and ±15% for the weak reflexions. Unobserved reflexions were assigned intensities of half the smallest observed intensity in a given layer. No absorption corrections were applied ($\mu R = 0{\cdot}23$ for the *c*-axis mounting).

Normalized structure factors ($E$ values) were computed by the $K$ curve method (Karle, Hauptman & Christ, 1958) which establishes scale and temperature corrections for the observed structure factors. Table 1 shows the experimental values for several functions of the normalized structure factors compared with the corresponding theoretical values for centrosymmetric and non-centrosymmetric structures respectively. The overall implication of these results is that the structure is centric, and the crystals were accordingly assigned to space group $P\bar{1}$.

Table 1. *Statistical distributions and averages, experimental and theoretical*

| | Experimental % | Centrosym. % | Non-centrosym. % |
|---|---|---|---|
| $\|E\|>3$ | 0·200 | 0·30 | 0·01 |
| $\|E\|>2{\cdot}5$ | 0·900 | 1·24 | 0·19 |
| $\|E\|>2$ | 2·700 | 5·00 | 1·80 |
| $\|E\|>1$ | 33·700 | 32·00 | 36·80 |
| $\langle\|E\|\rangle$ | 0·848 | 0·798 | 0·886 |
| $\langle\|E^2\|\rangle$ | 0·994 | 1·000 | 1·000 |
| $\langle\|F\|^2\rangle$ / $\langle I\rangle$ | 0·609 | 0·637 | 0·787 |

## Determination of the structure

The structure was solved by the symbolic addition procedure (Karle & Karle, 1963) for the centrosymmetric case, using programs prepared for the London University Atlas computer. Heavy atom and Patterson superposition techniques were subsequently employed both as independent checks on the results of the direct determination, and also for the purpose of testing other computer programs. In this way the relative merits of the three methods were assessed for the present case.

*Direct phase determination*

The sign of the 040 reflexion was established by use of the $\Sigma_1$ formula for space group $P\bar{1}$ (Hauptman & Karle, 1953*b*),

$$sE_{2\mathbf{h}} \sim s(E_{\mathbf{h}}^2 - 1)\,. \tag{1}$$

This indicated that the sign of 040 was positive with a probability of 0·99, computed from

$$P+(E_{2\mathbf{h}}) = \tfrac{1}{2} + \tfrac{1}{2}\tanh\{(\sigma_3/2\sigma_2^{3/2})\,|E_{2\mathbf{h}}|\,(|E_{\mathbf{h}}|^2 - 1)\} \tag{2}$$

where $\sigma_n = \sum_{j=1}^{N} Z_j^n$, $Z_j$ being the atomic number of the $j$th atom in a unit cell containing $N$ atoms. In order to apply the $\Sigma_2$ formula (Zachariasen, 1952; Hauptman & Karle, 1953*b*),

$$sE_{\mathbf{h}} \sim s \sum_{\mathbf{k}} E_{\mathbf{k}} E_{\mathbf{h}-\mathbf{k}}\,, \tag{3}$$

the 163 reflexions for which $|E| > 1{\cdot}5$ were arranged in descending order of magnitude in a $\Sigma_2$ listing program. For each reflexion **h** in turn the program determines and prints out all pairs of reflexions of the type **k** and **h**−**k** together with the corresponding product $|E_{\mathbf{h}}|\,|E_{\mathbf{k}}|\,|E_{\mathbf{h}-\mathbf{k}}|$, which is used, as described below, in assessing probabilities.

The phase determining procedure was then initiated by selecting three origin specifying reflexions which were arbitrarily allocated positive signs. The three reflexions chosen had high $|E|$ values and entered into many vector combinations in the $\Sigma_2$ listings, while at the same time conforming to the requirements that they belong to three different and linearly independent parity groups (Hauptman & Karle, 1953; Woolfson, 1961). At several stages of the subsequent analysis it became necessary to represent the sign of a selected reflexion, having a large $|E|$ value and long $\Sigma_2$ listing, by a letter (denoting + or −). Altogether five letter phases, *a*, *b*, *c*, *d* and *e* respectively, as shown in Table 2, were allocated.

Table 2. *Basic phase assignments used in application of the symbolic addition procedure*

| *h* | *k* | *l* | Sign | $\|E\|$ |
|---|---|---|---|---|
| 9 | $\bar{1}$ | $\bar{4}$ | + | 2·97 |
| 8 | $\bar{1}$ | $\bar{5}$ | + | 3·00 |
| 1 | $\bar{4}$ | 0 | + | 2·38 |
| 0 | 4 | 0 | + | 2·27 |
| 0 | 2 | 0 | *a* | 4·50 |
| 2 | 5 | 3 | *b* | 2·24 |
| 8 | 2 | 2 | *c* | 2·71 |
| 3 | 0 | 3 | *d* | 2·69 |
| 0 | 2 | 3 | *e* | 2·28 |

The application of equation (3) was carried out in two stages, maintaining a probability level in each case of $P+(E_{\mathbf{h}}) \geq 0{\cdot}95$ determined from the formula

$$P+(E_{\mathbf{h}}) = \tfrac{1}{2} + \tfrac{1}{2}\tanh\{(\sigma_3/\sigma_2^{3/2})\,|E_{\mathbf{h}}| \sum_{\mathbf{k}} E_{\mathbf{k}} E_{\mathbf{h}-\mathbf{k}}\} \tag{4}$$

(Hauptman & Karle, 1953*c*; Woolfson, 1954).

In the first stage the summations appearing in (3) and (4) were allowed to degenerate into single terms, corresponding to the basic sign relationship

$$sE_{\mathbf{h}} \sim sE_{\mathbf{k}} sE_{\mathbf{h}-\mathbf{k}} \tag{5}$$

with associated probability

$$P+(E_{\mathbf{h}}) = \tfrac{1}{2} + \tfrac{1}{2}\tanh\{(\sigma_3/\sigma_2^{3/2})\,|E_{\mathbf{h}}|\,|E_{\mathbf{k}}|\,|E_{\mathbf{h}-\mathbf{k}}|\,. \tag{6}$$

The value of $(\sigma_3/\sigma_2^{3/2})$ appearing in (4) was 0·091 in the present case, and it follows that a probability of 0·95 corresponds to terms for which $|E_{\mathbf{h}}| \sum_{\mathbf{k}} |E_{\mathbf{k}}|\,|E_{\mathbf{h}-\mathbf{k}}| \geq 8{\cdot}22$. It follows that the probability level adopted would hold even for single terms for which $|E_{\mathbf{h}}|\,|E_{\mathbf{k}}|\,|E_{\mathbf{h}-\mathbf{k}}| \geq 8{\cdot}22$. Terms satisfying this condition were found by inspection of the $\Sigma_2$ listings. Letter phases were

then introduced as needed for suitable reflexions, followed by substitution of the appropriate letter phase or + sign for as many terms as possible before introducing a new letter. In this way the phases of 96 reflexions were determined as various combinations of the six basic symbols appearing in Table 2.

In the second stage of the process, in order to determine additional phases without introducing more letters or reducing the probability, it was necessary to include multiple terms in the summations appearing in equations (3) and (4). This was achieved by writing the 96 known phase symbols into the $\Sigma_2$ listings and noting the resulting phase combinations. Table 3 shows the listing for the reflexion $9\bar{8}6$ with the phases written in. There is a strong indication that the phase in this case is *abd* (shown by 4 indications out of 5). In general, a given indication was accepted only if it occurred at least three or four times, the appropriate phase symbol being then added to the list. In this way a further 53 phases were assigned. An important feature of the above analysis was that it revealed a number of frequently occurring relationships between the letters, some of which had high individual probabilities computed from equation (6). The most significant relationships, given in Table 4, reduce to $a=b=ec$ and $d=c$. Combined with weaker indications that $e=+$ (with a maximum probability of 0·81) two solutions result, namely $a=b=c=d=e=+$ or $a=b=c=d=-$, $e=+$. The first solution corresponds to a complete phase set consisting of all + signs, which always results when the three origin specifying reflexions are designated +. Since such a phase distribution implies the existence of an atom at the origin, which was hardly possible in the present case, the second solution was chosen as being most probable.

An additional ten phases were determined by extending the analysis to include reflexions in the range $1{\cdot}5 \geq |E_{\mathbf{h}}| \geq 1{\cdot}45$, at which point a total of 159 phases had been assigned, equivalent to about 8 phases per atom (excluding hydrogen). An *E* map (Karle, Hauptman, Karle & Wing, 1958) computed with the 159 terms at intervals of 1/30 along each axis clearly revealed the structure in spite of three spurious peaks just above background. Composite sections of the *E* map in the *ac* plane are shown superposed in Fig. 1. An electron density map using phases for the complete data calculated from the positions indicated in Fig. 1 confirmed the positions of the water molecules. Refinement of the structure is described in a later section.

Table 4. *The most frequently occurring relationships between letters*

| Relationship | Highest probability |
|---|---|
| $ac=e$ | 0·94 |
| $c=eb$ | 0·94 |
| $b=ed$ | 0·93 |
| $ad=e$ | 0·90 |
| $ab=cd$ | 0·95 |

*Heavy atom method*

A sharpened Patterson function calculated at intervals of 1/30 along each axis contained two dominant peaks. The P–P vector was identified from the tetrahedral distribution of P–O peaks around it, and the other strong peak at 2·7 Å from the origin was attributable to several near-coincident interatomic vectors from the organic part of the molecule.

The electron density map, calculated with phases based on the phosphorus positions alone, revealed most of the molecule as peaks above background, but with less clarity than that of the first *E* map. Although about 65% of the phases were correctly determined from the phosphorus atom, the lack of resolution was probably due to the introduction of a number of large terms with reversed signs. The use of a weighting scheme, such as that of Sim (1961), to improve the map was not investigated. All Fourier calculations up to this

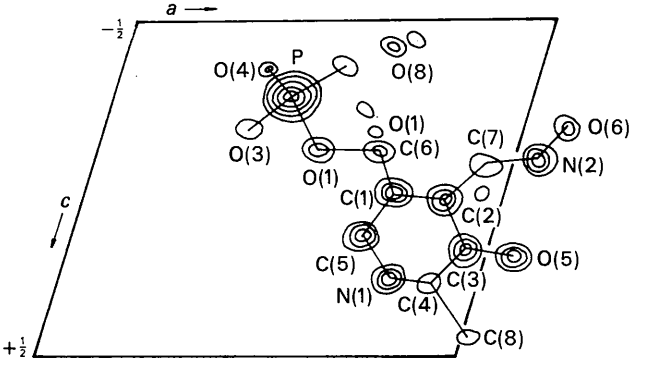


Fig. 1. Pyridoxal phosphate oxime, superposed sections in the *ac* plane of the three-dimensional *E* map.

Table 3. $\Sigma_2$ *listing for the reflexion* $9\bar{8}6$ *with appropriate phase symbols added*

| k | | | $\lvert E_{\mathbf{k}}\rvert$ | h−k | | | $\lvert E_{\mathbf{h}-\mathbf{k}}\rvert$ | $\lvert E_{\mathbf{h}}\rvert$ $\lvert E_{\mathbf{k}}\rvert$ $\lvert E_{\mathbf{h}-\mathbf{k}}\rvert$ |
|---|---|---|---|---|---|---|---|---|
| 1 | −5 | 0 | *bd* 2·16 | 8 | −3 | −6 | *a* 1·63 | *abd* 6·40 |
| 10 | −2 | −2 | *ab* 2·04 | 1 | 6 | 4 | *d* 1·88 | *abd* 6·97 |
| 10 | −7 | −1 | *d* 1·87 | 1 | 1 | 5 | *ab* 1·63 | *abd* 5·54 |
| 4 | −8 | −3 | *d* 1·83 | 5 | 0 | −3 | *ecd* 1·58 | *ec* 5·25 |
| 3 | −9 | −4 | 1·76 | 6 | 1 | −2 | 1·58 | 5·03 |
| 3 | −5 | −6 | 1·70 | 6 | −3 | 0 | 1·51 | 4·66 |
| 6 | −7 | −2 | 1·68 | 3 | −1 | −4 | 1·63 | 4·98 |
| 10 | −4 | −2 | *b* 1·62 | 1 | 4 | 4 | *ad* 1·67 | *abd* 4·93 |
| 0 | −2 | 0 | *a* 4·50 | 9 | −6 | −6 | 1·73 | 14·08 |
| 0 | −8 | 0 | +2·48 | 9 | 0 | −6 | 1·85 | 8·30 |

stage of the work were made on the London University Atlas computer using Dollimore's (1966) program.

*Superposition method*

The minimum function, $M_2$ (Buerger, 1959) was computed from the sharpened Patterson function using the two phosphorus positions in the unit cell as superposition points. The sharpening function used here and in the above section was $s^2 \exp(-0{\cdot}17s^2)$, where $s=2\sin\theta$ (Fischman, MacGillavry & Romers, 1961). Grid intervals of 50ths along **a**, 30ths along **b** and 40ths along **c** were used, with no interpolation between grid points in the superposition routine. The results compare favourably with those of the previous methods, $M_2$ showing better relative peak heights than the heavy atom electron density map but containing several spurious peaks as well.

Of the three preliminary density functions calculated the $E$ map gave the clearest and most unambiguous representation of the structure. The heavy atom Fourier and minimum function $M_2$ were both interpretable but contained a greater number of imperfections. These observations are summarized in Table 5.

Table 5. *Comparison of the three preliminary density functions*

All three maps showed the requisite number of peaks in the right places but with different spuriosities and characteristics listed in the Table.

| Technique | Number of spurious peaks | Atomic sites represented weakly (*i.e.* only just above background) |
|---|---|---|
| $E$ map | 3 | O(2), O(3)<br>C(4)<br>C(7), C(8)<br>O(7) |
| Heavy atom Fourier (unweighted) | 4 | All except P |
| $M_2$ function | 6 | C(1), C(2), C(4)<br>N(1) |

Table 6. *Final coordinate parameters together with their standard deviations*

| | $x$ | $\sigma(x)$ | $y$ | $\sigma(y)$ | $z$ | $\sigma(z)$ |
|---|---|---|---|---|---|---|
| P | 0·4267 | 0·0003 | 0·8676 | 0·0005 | −0·2610 | 0·0005 |
| O(1) | 0·5187 | 0·0008 | 0·7423 | 0·0014 | −0·1107 | 0·0011 |
| O(2) | 0·5156 | 0·0009 | 1·0885 | 0·0013 | −0·3639 | 0·0012 |
| O(3) | 0·3225 | 0·0008 | 0·8364 | 0·0015 | −0·1738 | 0·0018 |
| O(4) | 0·3609 | 0·0009 | 0·7557 | 0·0015 | −0·3731 | 0·0013 |
| C(6) | 0·6452 | 0·0013 | 0·7511 | 0·0019 | −0·1332 | 0·0016 |
| C(1) | 0·7425 | 0·0012 | 0·7442 | 0·0018 | 0·0263 | 0·0017 |
| C(2) | 0·8729 | 0·0011 | 0·7378 | 0·0018 | 0·0419 | 0·0017 |
| C(3) | 0·9586 | 0·0012 | 0·7405 | 0·0017 | 0·1832 | 0·0015 |
| C(4) | 0·9164 | 0·0013 | 0·7464 | 0·0020 | 0·3068 | 0·0019 |
| N(1) | 0·7872 | 0·0011 | 0·7422 | 0·0017 | 0·2836 | 0·0015 |
| C(5) | 0·7003 | 0·0012 | 0·7433 | 0·0018 | 0·1480 | 0·0016 |
| C(7) | 0·9144 | 0·0011 | 0·7343 | 0·0018 | −0·0870 | 0·0019 |
| N(2) | 1·0420 | 0·0010 | 0·7577 | 0·0015 | −0·0783 | 0·0013 |
| O(6) | 1·0675 | 0·0009 | 0·7576 | 0·0016 | −0·2107 | 0·0012 |
| O(5) | 1·0891 | 0·0008 | 0·7476 | 0·0013 | 0·2086 | 0·0017 |
| C(8) | 1·0068 | 0·0016 | 0·7577 | 0·0022 | 0·4601 | 0·0016 |
| O(7) | 0·6450 | 0·0012 | 0·3246 | 0·0016 | −0·1860 | 0·0014 |
| O(8) | 0·6845 | 0·0011 | 0·7033 | 0·0016 | −0·4682 | 0·0013 |

Table 7. *Final anisotropic temperature factors together with their standard deviations*

$\beta_{ij}=2\pi^2 a_i^* a_j^* U_{ij}$ .

| | $\beta_{11}$ | $\beta_{22}$ | $\beta_{33}$ | $2\beta_{23}$ | $2\beta_{32}$ | $2\beta_{12}$ |
|---|---|---|---|---|---|---|
| P | 0·0062 (3) | 0·0248 (9) | 0·0147 (6) | −0·0166 (12) | 0·0004 (6) | 0·0110 (8) |
| O(1) | 0·0092 (10) | 0·0364 (31) | 0·0139 (17) | −0·0127 (36) | 0·0015 (19) | 0·0201 (28) |
| O(2) | 0·0119 (11) | 0·0211 (24) | 0·0181 (19) | −0·0128 (34) | 0·0099 (22) | 0·0098 (27) |
| O(3) | 0·0083 (10) | 0·0412 (34) | 0·0179 (19) | −0·0238 (40) | 0·0026 (20) | 0·0167 (30) |
| O(4) | 0·0116 (11) | 0·0303 (31) | 0·0219 (22) | −0·0333 (42) | 0·0025 (24) | 0·0025 (31) |
| C(6) | 0·0078 (13) | 0·0266 (36) | 0·0134 (25) | −0·0108 (48) | 0·0041 (26) | 0·0149 (35) |
| C(1) | 0·0087 (13) | 0·0206 (35) | 0·0168 (28) | −0·0182 (49) | 0·0033 (27) | 0·0094 (35) |
| C(2) | 0·0069 (12) | 0·0247 (36) | 0·0188 (27) | −0·0291 (52) | −0·0012 (27) | 0·0098 (33) |
| C(3) | 0·0106 (13) | 0·0163 (32) | 0·0116 (23) | −0·0074 (43) | 0·0033 (27) | 0·0111 (34) |
| C(4) | 0·0097 (14) | 0·0235 (37) | 0·0222 (30) | −0·0209 (57) | 0·0035 (33) | 0·0123 (37) |
| N(1) | 0·0119 (13) | 0·0226 (32) | 0·0206 (24) | −0·0188 (44) | 0·0048 (28) | 0·0130 (33) |
| C(5) | 0·0105 (14) | 0·0147 (31) | 0·0146 (26) | −0·0096 (44) | 0·0031 (27) | 0·0091 (34) |
| C(7) | 0·0080 (13) | 0·0182 (34) | 0·0161 (27) | −0·0069 (51) | 0·0082 (28) | 0·0101 (34) |
| N(2) | 0·0086 (11) | 0·0207 (28) | 0·0166 (22) | −0·0167 (41) | 0·0051 (24) | 0·0082 (28) |
| O(6) | 0·0099 (10) | 0·0438 (34) | 0·0187 (19) | −0·0340 (44) | −0·0007 (22) | 0·0178 (30) |
| O(5) | 0·0073 (8) | 0·0263 (25) | 0·0157 (17) | −0·0141 (35) | 0·0002 (19) | 0·0123 (25) |
| C(8) | 0·0183 (20) | 0·0314 (43) | 0·0073 (23) | −0·0249 (22) | −0·0047 (33) | 0·0149 (49) |
| O(7) | 0·0023 (17) | 0·0266 (30) | 0·0225 (24) | −0·0193 (43) | 0·0096 (32) | 0·0148 (37) |
| O(8) | 0·0189 (15) | 0·0361 (33) | 0·0196 (21) | −0·0184 (42) | 0·0067 (31) | 0·0301 (35) |

### Refinement of the structure

The structure was refined by block-diagonal least-squares methods with a program supplied by Dr R.D. Diamand (Diamand & Drew, 1966). The function minimized was $\sum_{hkl} \omega(|F_o|-|F_c|)^2$. An overall scale factor is incorporated in $|F_o|$ and refined during the course of the calculations. The weighting scheme used was that of Hughes (1941) with

$$\omega^{1/2}=1 \text{ for } |F_o|<|F^*|$$
$$\omega^{1/2}=|F^*|/|F_o| \text{ for } |F_o|\geq|F^*|,$$

where $|F^*|$ was taken as the mean of all $|F_o|$. Atomic scattering factors were taken from *International Tables for X-ray Crystallography* (1962). Unobserved reflexions were not included in these calculations.

Six cycles of refinement in which positional parameters and individual isotropic temperature factors were varied, reduced the conventional $R$ value from 38% to 14%. After a further eight cycles with anisotropic temperature factors the refinement was stopped with $R=11\%$, no significant changes occurring in the final cycle. Further reduction in $R$ might have been achieved by refinement of individual $c$ axis Weissenberg level scale factors and also by inclusion of hydrogen positions neither of which was attempted. The atomic parameters and estimated errors from the final least-squares cycle are given in Tables 6 and 7, and tables of $F_o$ and $F_c$ may be obtained from the authors.

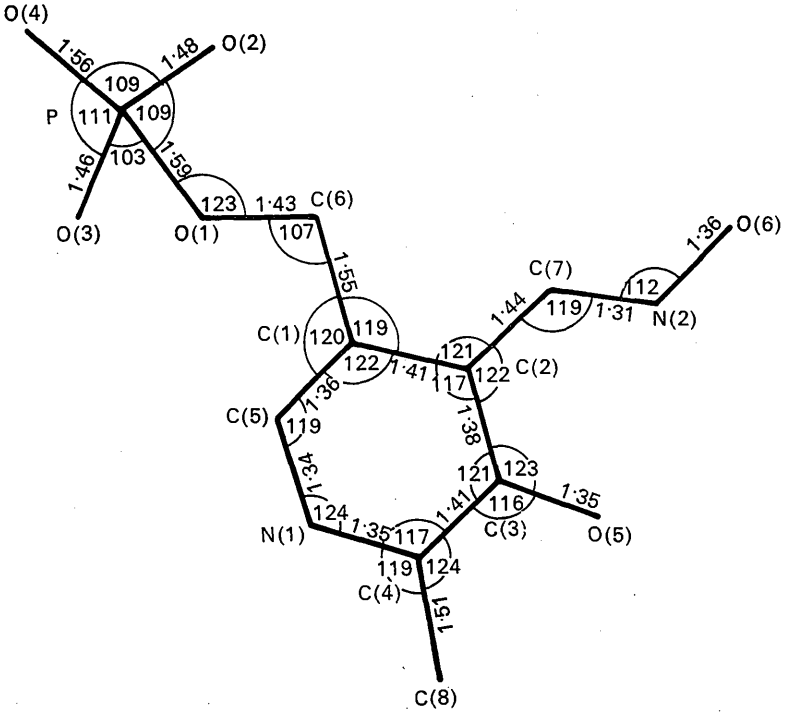


Fig. 2. Pyridoxal phosphate oxime, bond lengths and angles.

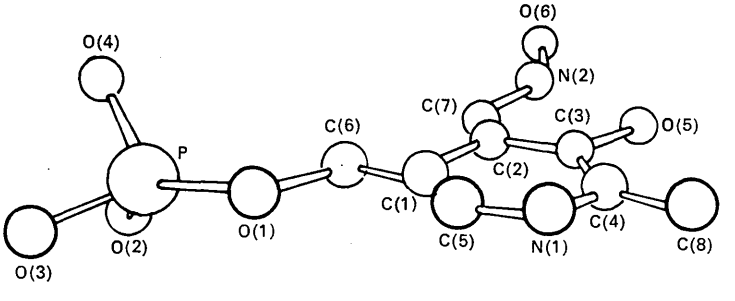


Fig. 3. Pyridoxal phosphate oxime, molecular configuration viewed at about 10° to the plane of the ring.

## Description of the structure

### *Molecular configuration*

Bond lengths and angles corresponding to the positional parameters from the final least-squares cycle are listed in Tables 8 and 9 and shown in Fig. 2. With the exception of phosphate group atoms P, O(2), O(3) and O(4), the molecule is to a good approximation planar. A view of a model of the molecule is illustrated in Fig. 3. The molecular configuration is influenced by a close contact between atoms O(5) and N(2), suggesting the presence of a strong intramolecular hydrogen bond (2·56 Å).

Table 8. *Interatomic distances in pyridoxal phosphate oxime*

| Bond | Bond length (Å) | e.s.d. (Å) |
|---|---|---|
| P —O(1) | 1·59 | (0·01) |
| P —O(2) | 1·48 | (0·01) |
| P —O(3) | 1·46 | (0·01) |
| P —O(4) | 1·56 | (0·01) |
| O(1)–C(6) | 1·43 | (0·02) |
| C(6)–C(1) | 1·55 | (0·02) |
| C(1)–C(2) | 1·41 | (0·02) |
| C(2)–C(3) | 1·38 | (0·02) |
| C(3)–C(4) | 1·41 | (0·02) |
| C(4)–N(1) | 1·35 | (0·02) |
| N(1)–C(5) | 1·34 | (0·02) |
| C(5)–C(1) | 1·36 | (0·02) |
| C(2)–C(7) | 1·44 | (0·02) |
| C(7)–N(2) | 1·31 | (0·02) |
| N(2)–O(6) | 1·36 | (0·02) |
| C(3)–O(5) | 1·35 | (0·02) |
| C(4)–C(8) | 1·51 | (0·02) |

The crystal structure is based upon a complex network of hydrogen bonds involving the two water molecules and various constituents of the pyridoxal phosphate oxime molecule.

### *The phosphate group*

The P–O bond lengths in pyridoxal phosphate oxime correspond to values found in other organic phosphates, as summarized by Karle & Britts (1966). The bond length of 1·58 Å for P–O(1) conforms to the P–OR classification, and the P–O(4) bond length of 1·56 Å appears to belong to the P–OH group. The two shorter bonds P–O(2), which is 1·48 Å, and P–O(3) which is 1·46 Å, are both less than the mean P–O bond length of 1·505 Å, P–O(3) significantly so. Both O(2) and O(3) are hydrogen bonded to water molecules, an effect which may be responsible for the shortening of the corresponding P–O bonds. The existence of a short P–O bond has been reported by Dunitz & Rollett (1956) in dibenzylphosphoric acid, in which the oxygen atom also takes part in intermolecular hydrogen bonding.

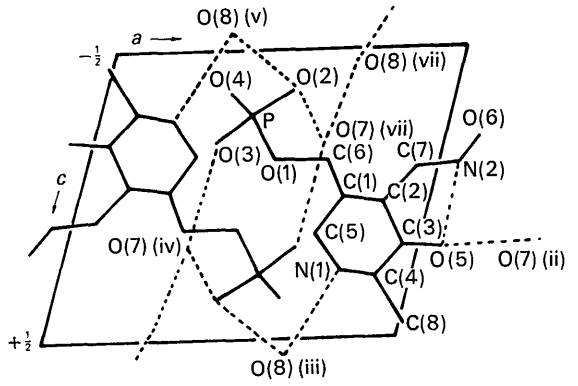


Fig. 4. Pyridoxal phosphate oxime, proposed hydrogen bond network represented diagrammatically from superposed sections in the *ac* plane of the three-dimensional electron density map.

Table 9. *Bond angles in pyridoxal phosphate oxime*

| Atoms | Angle | e.s.d. |
|---|---|---|
| O(4)–P —O(2) | 108·7° | (0·6)° |
| O(4)–P —O(3) | 110·7 | (0·6) |
| O(3)–P —O(1) | 103·1 | (0·6) |
| O(2)–P —O(1) | 109·0 | (0·6) |
| O(4)–P —O(1) | 107·1 | (0·5) |
| O(3)–P —O(2) | 117·6 | (0·6) |
| P —O(1)–C(6) | 123·4 | (0·8) |
| C(6)–C(1)–C(5) | 119·5 | (1·1) |
| C(6)–C(1)–C(2) | 118·9 | (1·1) |
| C(5)–C(1)–C(2) | 121·6 | (1·2) |
| C(1)–C(2)–C(3) | 117·0 | (1·2) |
| C(1)–C(2)–C(7) | 120·7 | (1·2) |
| C(2)–C(3)–C(4) | 121·3 | (1·3) |
| C(2)–C(3)–O(5) | 123·0 | (1·2) |
| C(4)–C(3)–O(5) | 115·6 | (1·2) |
| C(3)–C(4)–N(1) | 116·9 | (1·3) |
| C(3)–C(4)–C(8) | 123·8 | (1·2) |
| C(8)–C(4)–N(1) | 119·3 | (1·2) |
| C(4)–N(1)–C(5) | 124·4 | (1·3) |
| N(1)–C(5)–C(1) | 118·6 | (1·3) |
| C(2)–C(7)–N(2) | 118·2 | (1·3) |
| C(7)–N(2)–O(6) | 118·8 | (1·1) |
| O(1)–C(6)–C(1) | 107·1 | (1·1) |
| C(3)–C(2)–C(7) | 122·3 | (1·3) |

### *The pyridine ring*

The pyridine ring is planar within experimental error. Table 10 lists the deviations of the individual atoms from the least-squares plane of the ring, together with their standard deviations perpendicular to the plane. The equation of the least-squares plane through the ring atoms, expressed in direct space coordinates is

$$0{\cdot}007x+0{\cdot}875y-0{\cdot}484z=4{\cdot}714\ .$$

Thanks are due to Dr J. Milledge for making this calculation.

Table 10. *Distances of ring atoms from mean plane and their standard deviations in direction perpendicular to the plane*

| | Distance from plane (Å) | Standard deviation $\sigma_\perp$ (Å) |
|---|---|---|
| C(1) | 0·018 | 0·015 |
| C(2) | −0·014 | 0·015 |
| C(3) | −0·002 | 0·015 |
| C(4) | −0·004 | 0·014 |
| N(1) | 0·019 | 0·017 |
| C(5) | −0·015 | 0·014 |

The valence angle at the nitrogen atom, C(4)–N(1)–C(5), is 124·4 ± 1·3°, which is significantly greater than 120°, as found in the other pyridine derivatives. This effect has been attributed to the removal of $\pi$ electrons from three positions in the ring by the nitrogen atom (Hanic, 1966).

*Hydrogen bonds*

The proposed intermolecular system of hydrogen bonds is indicated in Figs. 4 and 5, and the corresponding bond lengths appear in Table 11. Symmetry operations used in generating neighbouring molecules are given in Table 12. The strong intermolecular hydrogen bond O(6)---O(3) (vi) of 2·53 Å is similar to that found in phosphoric acid (Furberg, 1955). All other hydrogen bonds involve the water molecules.

Table 11. *Intermolecular hydrogen bond distances*

| Bond | Distance (Å) |
|---|---|
| O(5)–O(7) (ii) | 3·29 |
| N(1)–O(8) (iii) | 2·71 |
| O(3)–O(7) (iv) | 2·87 |
| O(2)–O(7) (vii) | 2·82 |
| O(2)–O(8) (v) | 2·89 |
| O(8)–O(7) | 2·69 |
| O(6)–O(3) (vi) | 2·53 |

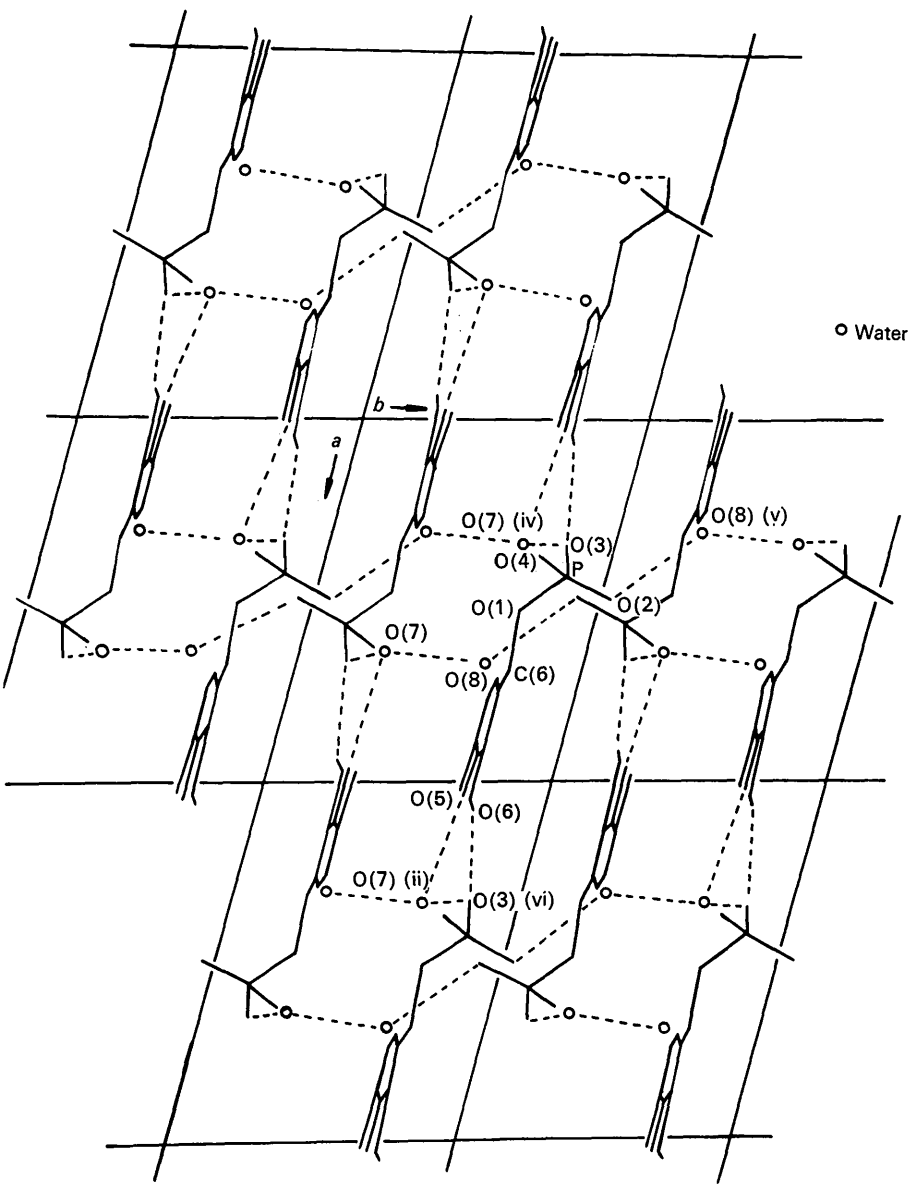


Fig. 5. Packing of the molecules and proposed hydrogen bonds illustrated from superposed sections in the *ab* plane of the three-dimensional electron density map.

Table 12. *Symmetry operations used to generate neighbouring molecules from coordinates of atoms in the asymmetric unit* (*Table* 6)

| | |
|---|---|
| (i) | $(-x, -y, -z)$ |
| (ii) | $(2-x, 1-y, -z)$ |
| (iii) | $(x, y, 1+z)$ |
| (iv) | $(1-x, 1-y, -z)$ |
| (v) | $(1-x, 2-y, -1-z)$ |
| (vi) | $(1+x, y, z)$ |
| (vii) | $(x, 1+y, z)$ |

The authors wish to thank Mrs J. Dollimore, Professor M. M. Woolfson and Dr R. D. Diamand for the use of their computer programs, and also Dr J. Milledge for carrying out one of the computations. All other computations were made using original programs. Thanks are also due to the Medical Research Council for the award of a Research Scholarship to one of us (A.N.B.) during the course of this work, a more complete account of which is given elsewhere (Barrett, 1967). We also thank Dr S. J. Morris for growing the crystal specimens and Dr C. H. Carlisle for suggesting the problem.

### References

BARRETT, A. N. (1967). Ph. D. Thesis, University of London.
BUERGER, M. J. (1959). *Vector Space*. New York: John Wiley.
DIAMAND, R. D. & DREW, M. G .B. (1966). I.U.Cr. *World List of Crystallographic Computer Programs*, 3068. Utrecht: Oosthoek.
DOLLIMORE, J. (1966). *A Fourier Program for Luna*, Circular No. 1(2). Document No. LSP32, Univ. of London Atlas Computing Service.
DUNITZ, J. D. & ROLLETT, J. S. (1956). *Acta Cryst.* **9**, 327.
FISCHMANN, E., MACGILLAVRY, C. H. & ROMERS, C. (1961). *Acta Cryst.* **14**, 753.
FURBERG, S. (1955). *Acta Chem. Scand.* **9**, 1557.
HANIC, F. (1966). *Acta Cryst.* **21**, 332.
HAUPTMAN, H. & KARLE, J. (1953). *The Solution of the Phase Problem. I. The Centrosymmetric Crystal.* A.C.A. Monograph No. 3, New York: Polycrystal Book Service. (*a*) p. 12, (*b*) pp. 46 and 47, (*c*) pp. 39–43.
HUGHES, E. W. (1941). *J. Amer. Chem. Soc.* **63**, 1741.
*International Tables for X-ray Crystallography* (1962). Vol. III, pp. 202–203. Birmingham: Kynoch Press.
KARLE, I. L. & BRITTS, K. (1965). *Z. Kristallogr.* **121**, 2/4, p. 191.
KARLE, I. L., HAUPTMAN, H., KARLE, J. & WING, A. B. (1958). *Acta Cryst.* **11**, 257.
KARLE, J., HAUPTMAN, H. & CHRIST, C. L. (1958). *Acta Cryst.* **11**, 757.
KARLE, I. L. & KARLE, J. (1963). *Acta Cryst.* **16**, 969.
MAIN, P. & WOOLFSON, M. M. (1963). *Acta Cryst.* **16**, 731.
RABINOWITZ, J. C. & SNELL, E. E. (1948). *J. Biol. Chem.* **176**, 1157.
SIM, G. A. (1961). *Computing Methods and the Phase Problem in X-ray Crystal Analysis*. Oxford: Pergamon Press.
WOOLFSON, M. M. (1954). *Acta Cryst.* **7**, 61.
WOOLFSON, M. M. (1961). *Direct Methods in Crystallography*, p. 23. Oxford: Univ. Press.
ZACHARIASEN, W. H. (1952). *Acta Cryst.* **5**, 68.

*Acta Cryst.* (1969). B**25**, 695

# Crystallography of $Pr(ReO_4)_3 . 3H_2O$, Praseodymium Perrhenate Trihydrate

BY WILLIAM G. R. DE CAMARGO
*Department of Mineralogy, University of S. Paulo, SP, Brazil*

AND C. R. LEITE
*Faculdade de Filosofia, Ciências e Letras, Araraquara, SP, Brazil*

(*Received* 11 *January* 1968)

The monoclinic crystals of praseodymium perrhenate trihydrate have a well developed {100} pinacoid form, and poorly developed remaining crystallographic forms: {001}, {011}, {012}, {102}, {$\bar{1}$02}, {110} and {$\bar{1}$12}. The crystallographic constants could be computed from the observed interfacial angles: $a:b:c = 1{\cdot}539:1:2{\cdot}141$ and $\beta = 86°03'$. The crystals are light green, with no appreciable pleochroism, presenting the following optical constants: $X = \alpha = 1{\cdot}678$; $b = Y = \beta = 1{\cdot}688$; $Z = \gamma = 1{\cdot}690$; $Z \wedge c = 35°–40°$ and $2V_{calc}^{(+)} = 53°$. The unit-cell parameters, determined by precession photographs and refined by powder diagrams, resulted in the values: $a_0 = 11{\cdot}68$, $b_0 = 7{\cdot}47$, $c_0 = 16{\cdot}06$ Å and $\beta = 86°04'$, space group $P2_1/c$. With four molecules per unit cell the calculated specific gravity of 4·49 g.cm$^{-3}$ agrees very well with the observed one of 4·51 g.cm$^{-3}$.

Crystals of praseodymium perrhenate trihydrate, $Pr(ReO_4)_3 . 3H_2O$, synthesized for the first time by Giesbrecht, Perrier & Vicentini (1966) (in the Chemistry Department of the University of São Paulo, Brazil) have been the object of the crystallographic investigation reported in this paper.